UDC 629.5.03

M. I. LAMAS
J. D. RODRÍGUEZ
C. G. RODRÍGUEZ

CFD Analysis of Biologically--Inspired Marine Propulsors

Preliminary communication

In the present work, the design and testing of two propulsion mechanisms which emulate fish swimming are presented. The motivation comes from the high efficiency and maneuverality that fish demonstrate over conventional rotary propellers. In order to know the fluid flow pattern in detail, a 3D CFD model was developed. Details of the velocity and pressure fields were obtained, as well as the hydrodynamic forces, cruising velocity, power and efficiency. The results obtained using this CFD model were validated with the experimental prototypes, obtaining a reasonable agreement. Once validated, the CFD model was used to analyze several configurations of the propelling fin, obtaining that thunniform swimming mode is the most efficient.

Keywords: *CFD, fish swimming, marine propulsion*

Authors' address (Adresa autora):
Universidade da Coruña; *Escola Universitaria Politécnica*
Avda 19 de Febreiro s/n, 15405 Ferrol, A Coruña, Spain
e-mail: isabellamas@udc.es

Received (Primljeno): 2011-11-18
Accepted (Prihvaćeno): 2011-01-10

Open for discussion (Otvoreno za raspravu): 2013-06-30

CFD analiza biološki potaknutih brodskih propulzora

Prethodno priopćenje

U priloženom se radu prikazuje projektiranje i testiranje dvaju propulzijskih mehanizma koji oponašaju plivanje riba. Poticaj za ovo istraživanje potekao je od spoznaje o visokoj učinkovitosti i upravljivosti koju pokazuju ribe u odnosu na uobičajene rotirajuće propulzore. U cilju detaljnog upoznavanja slike strujanja razvijen je 3D CFD model. Dobiveni su detaljni podaci o poljima brzina i tlakova kao i hidrodinamičke sile, brzina krstarenja, snaga i učinkovitost. Rezultati dobiveni CFD modelom se dobro slažu s rezultatima sa pokusnim prototipovima. Ovako provjereni CFD model je potom iskorišten za analize nekoliko konfiguracija propulzijskih peraja pri čemu se pokazalo da je način plivanja tuna najučinkovitiji.

Ključne riječi: *CFD, propulzija broda, riblje plivanje*

1 Introduction

Fish swimming is the result of millions of years of evolutionary optimization. Natural selection has ensured that the locomotion of fish, although not necessarily optimal, is very efficient and adapted to their living environments. For this reason, it has inspired mechanisms for marine propulsion in the past years. What makes the high efficiency of a biologically-inspired mechanism is the manner in which it works. An undulating fin creates an efficient jet in the direction of thrust. However, a rotary propeller generates a jet that rotates in the direction of propeller rotation (perpendicular to the direction of motion), which consumes a lot of unproductive power.

Several designs of marine propulsors which emulate the locomotion of fish have been built since the 1990s. For example, Yamamoto *et al*. [1] constructed an oscillating fin and studied several shapes of the tail. Barret *et al*. [2] made a mechanism called RoboTuna, which replicates the shape of a tuna, including the caudal and two smaller attached fins. Kato [3] presented a fish-like robot equipped with a pair of two pectoral fins on both sides. Guo [4] also made a fish-like robot with two tails. Herr and Dennis [5] built a robot with a flexible tail actuated by two explanted frog semitendinosus muscles controlled by an embedded microcontroller. MacIver *et al*. [6] built a high maneuverable mechanism which emulates a knifefish. Clark and Smits [7] built a flexible fin which imitates the pectoral fin of a batoid fish. Low [8] constructed a vehicle using a fin-like mechanism which produces the undulations of a fin ray. Lamas *et al*. [9] made a propulsor capable of reproducing several undulating movements. These investigations provided a great progress in biologically-inspired marine propulsion, and most of them concluded that biologically-inspired mechanisms are more maneuverable, efficient and/or less noisy than classical rotary propellers. However, the design of an efficient mechanism requires a complete understanding of the fluid pattern. In this regard, CFD (Computational Fluid Dynamics) offers an important tool to study the fluid flow in detail. CFD is a branch of fluid mechanics based on the subdivision of the computational domain into small elements overlaying the whole domain. For each subdivision, the governing equations are solved using numerical methods.

In this work, two biologically-inspired marine propulsors are presented. In order to analyze these designs, a 3D CFD model was developed. Once validated with experimental data, the CFD model was employed to study several undulating movements and parameters.

2 Fish swimming modes

Figure 1 illustrates the fins of a fish. Most fish generate thrust using their body and/or caudal fin (BCF), while other fish use

their median and/or paired fins (MPF). According to the reviews of Sfakiotakis *et al*. [10], Cheng and Chahine [11] and Colgate [12], BCF swimming mode is faster, but less maneuverable and stable than MPF swimming mode.

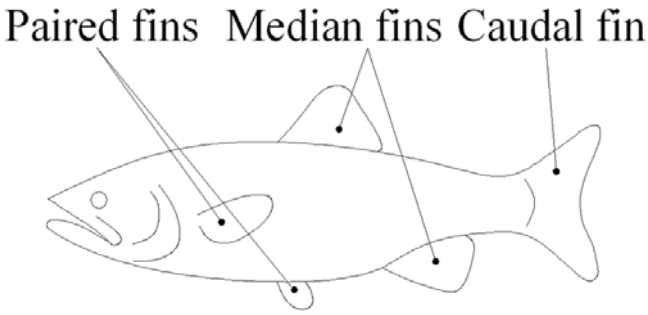

Figure 1 **Fins of a fish**
Slika 1 **Peraje ribe**

Some BCF swimming modes are shown in Figure 2. In anguilliform mode, undulation takes place along the whole body. Similar movements are observed in caranguiform mode, but with the amplitude undulations growing toward the tail. In thunniform mode the amplitude undulations also grows toward the tail, and practically take place in the posterior half of the fish. Ostraciiform locomotion is characterized by the pendulum-like oscillation of the (rather stiff) caudal fin, while the body remains essentially rigid.

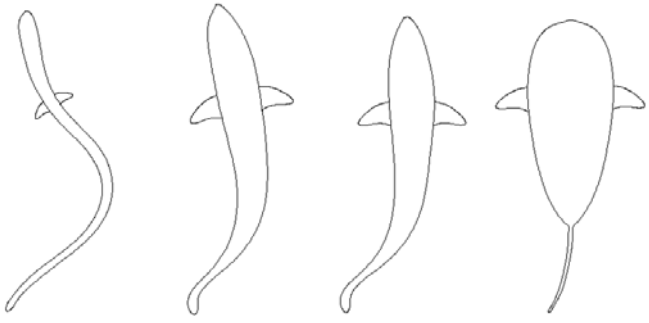

Figure 2 **Examples of BCF locomotion modes:**
(a) anguilliform
(b) caranguiform
(c) thunniform
(d) ostraciiform
Slika 2 **Primjeri načina plivanja korištenjem tijela i/ili repne peraje (BCF):**
(a) način plivanja riba iz reda Anguilliformes
(b) način plivanja riba iz reda Caranguiformes
(c) način plivanja riba iz reda Thunniformes
(d) način plivanja riba iz reda Ostraciiformes

On the other hand, some MPF swimming modes are shown in Figure 3. Rajiform, amiiform and gymnotiform modes are based on the movement of the pectoral, dorsal and anal fins respectively. In MPF swimming mode, propulsion is achieved by passing undulations along the fins, while the body remains practically rigid.

Figure 3 **Examples of MPF locomotion modes:**
(a) amiiform
(b) gymnotiform
(c) rajiform

Slika 3 **Primjeri načina plivanja korištenjem srednjih i/ili parnih peraja (MPF):**
(a) način plivanja riba iz reda Amiiformes
(b) način plivanja riba iz reda Gymnotiformes
(c) način plivanja riba iz reda Rajiformes

3 Mechanical designs

In order to study biologically-inspired marine propulsion, a mini catamaran (2.16 m long) was built. This is shown in Figure 4. An electric motor was situated above the ship in order to supply the power.

Figure 4 **Prototype used for trials**
Slika 4 **Prototip korišten u ispitivanjima**

Figure 5 **Schematic representation of the data acquisition system**
Slika 5 **Shematski prikaz sustava za prikupljanje podataka**

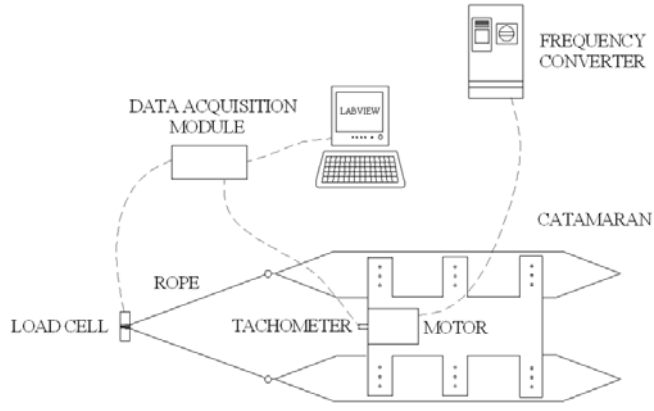

The data acquisition system is shown in Figure 5. The motor was connected to a frequency converter Altivar 58. A tachometer was installed at the motor shaft in order to measure the rotational speed. In order to measure the thrust, the catamaran was tied to an Utilcell 240 load cell by means of a rope. Both the measurements of the load cell and the tachometer were processed by a data acquisition module NI USB-6008, which sends the measurements to a computer. The results were analyzed by means of the software LabVIEW.

Two propelling mechanisms based on a 0.52 x 0.02 m fin were built. One of them was inspired by MPF movement and the other by BCF movement. The MPF mechanism is shown schematically in Figure 6 (a), and a photograph of the fin is shown in Figure 6 (b).

In this case, the undulating movement of the fin is guided by nine ribs. The principle of operation of each rib is shown in Figure 7. The crankshaft, moved by the motor, is connected to a rod and a connecting rod which pushes horizontally the rib tip. As the rib is fixed to a secondary axis, an oscillatory movement of amplitude $-\phi$, $+\phi$ is induced.

Figure 6 **MPF propulsor:**
(a) schematic representation
(b) photograph of the mechanism installed on the catamaran
Slika 6 **MPF propulzor:**
(a) shematski prikaz
(b) fotografija mehanizma ugrađenog na katamaran

(a)

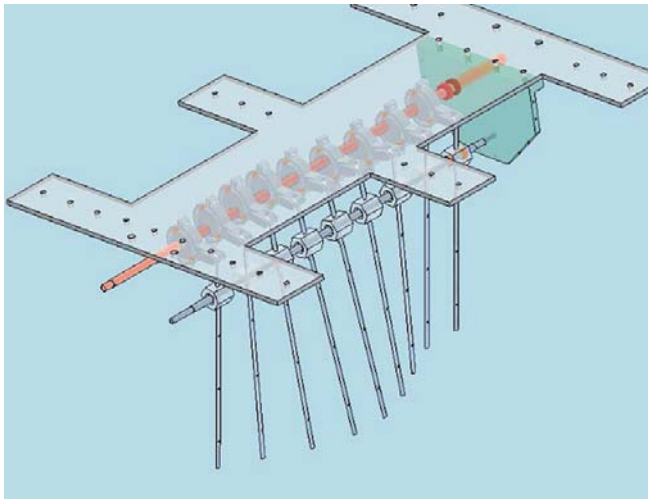

(b)

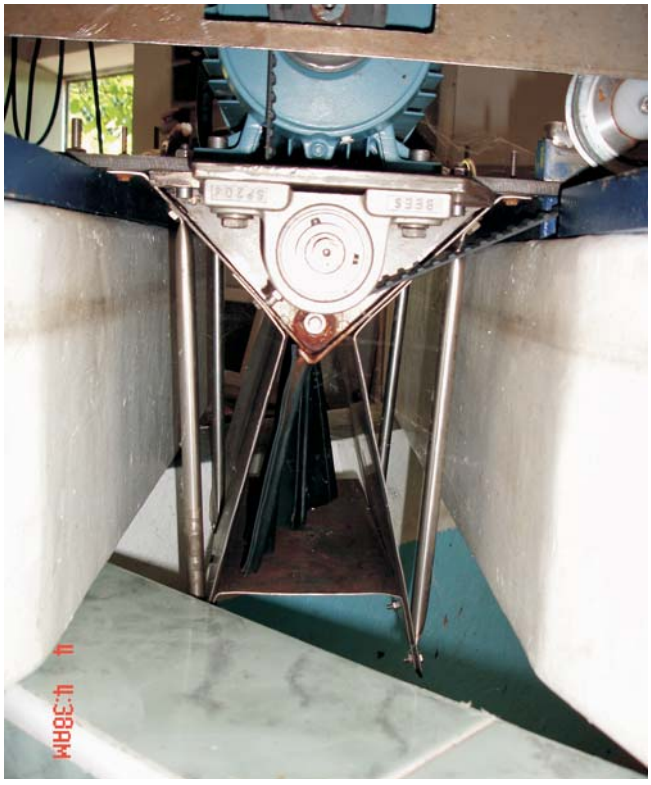

Figure 7 **Principle of operation of each rib**
Slika 7 **Princip rada svakog rebra**

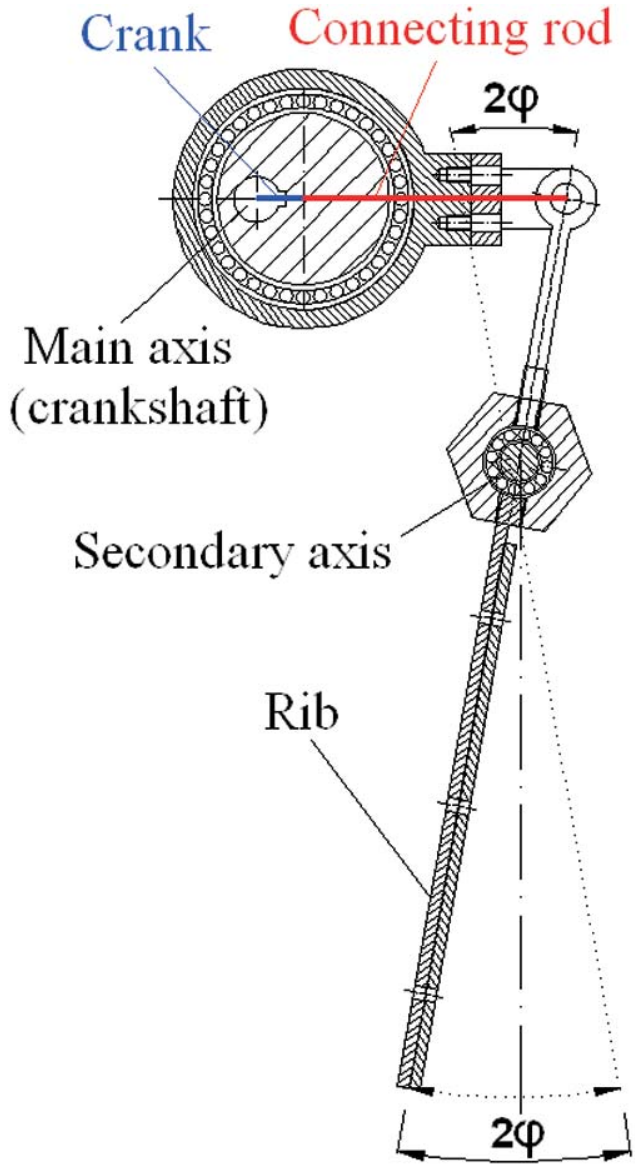

The other proposed mechanism is based on BCF locomotion. As can be seen in the schematic representation in Figure 8 (a), the undulating fin consists of eight rigid segments, each capable of relative rotation with respect to its neighbor links. The movement of each segment is generated by a camshaft situated above the fin. This camshaft can be modified to emulate anguilliform, caranguiform, thunniform and ostraciiform swimming modes. A photograph of the fin below the catamaran is shown in Figure 8 (b).

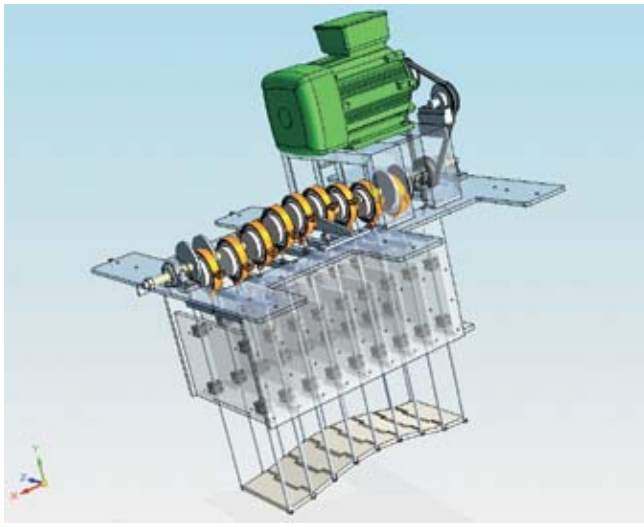

(a)

(b)

Figure 8 **BCF propulsor:**
(a) schematic representation
(b) photograph of the mechanism installed on the catamaran
Slika 8 **BCF propulzor:**
(a) shematski prikaz
(b) fotografija mehanizma ugrađenog na katamaran

4 Numerical procedure

In order to know the fluid flow in detail and optimize these designs, the two proposed mechanisms were studied using CFD. Four BCF swimming modes were analyzed. As MPF swimming mode is generally slower than BCF swimming mode, only gymnotiform movement was simulated. The undulating surfaces are schematically represented in Figure 9 and the details of the numerical procedure are shown in what follows.

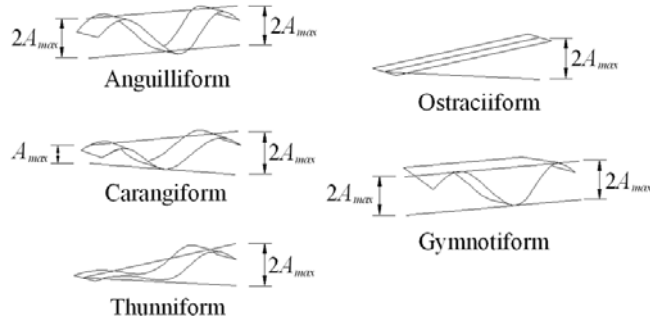

Figure 9 **Undulating patterns to study numerically**
Slika 9 **Valoviti obrasci za numeričko proučavanje**

4.1 Governing equations

The hydrodynamics of this problem is governed by RANS (Reynolds Averaged Navier-Stokes equations), *i.e.*, the continuity and momentum equations. Due to the high Reynolds numbers obtained (in most of the simulations, the Reynolds number exceeds 10^6), the flow was modeled as turbulent. Concerning the turbulence model, the standard k-ε was selected for its robustness, economy and reasonable accuracy for a wide range of cases.

The fin moves with a certain advancing velocity. If this problem was solved in a fixed coordinate system, it would require a large domain to accurately represent the advancing position of the fin, making the computation time very large. A usual approach used to save computational time is working in a coordinate system that moves with the investigate object. Particularly, in this work the fin was fixed at zero advancing velocity (it undulates but does not advance) and water was imposed to enter and leave the computational domain at the free-stream velocity, u_∞. Under such approach, the boundary conditions are those shown schematically in Figures 9 (a) and (b) for anguilliform and gymnotiform swimming modes respectively. There is an inlet and an outlet surface. The fin was treated as a no-slip undulating wall, while the top and bottom boundaries were modeled as slip walls. The four BCF swimming modes analyzed are symmetrical. On the other hand, gymnotiform MPF swimming mode is not symmetrical.

4.2 Computational mesh

Figures 10 (a) and (b) show the meshes used to simulate anguilliform and gymnotiform swimming modes respectively. In these figures, the front surface and the internal mesh were omitted for clarity. The meshes employed to simulate caranguiform, thunniform and ostraciiform swimming modes are similar to those shown in Figure 10 (a), so they are not represented. The gymnotiform mesh has 1200000 elements and the other meshes have 600000 elements due to the symmetry. The elements employed are triangular, and the size mesh is finer on the fin surface and in the wake region.

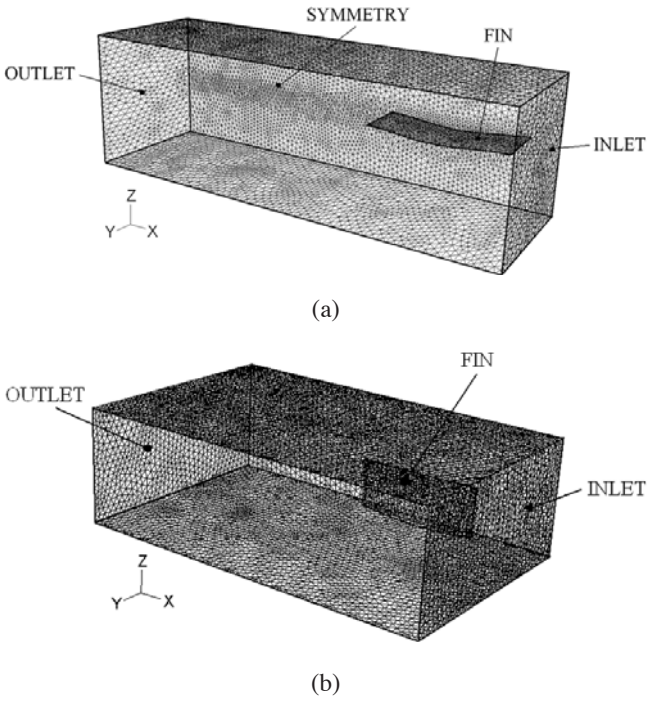

Figure 10 **Computational mesh:**
(a) anguilliform swimming mode
(b) gymnotiform swimming mode
Slika 10 **Računska mreža:**
(a) način plivanja riba iz reda Anguilliformes
(b) način plivanja riba iz reda Gymnotiformes

4.3 Numerical methodology

The simulations carried out in the present work were performed using the commercial software Ansys Fluent 6.3, based on the finite volume method. Pressure-velocity coupling was achieved using the PISO algorithm. A second order scheme was used for the discretization of convective terms and an implicit scheme was employed for the time integration. The time step was constant, 0.001 s.

In order to reach a situation which periodically repeats, *i.e.*, a quasi-steady state, it was necessary to study a long enough interval of time. For the cases studied, it was verified that this state is achieved after approximately twenty fin oscillation periods (from the 20th period of time, the results analyzed practically remain unchanged). For this reason, all the results carried out in the present paper correspond to the 20th period of time.

5 Results

5.1 Wake pattern, forces and validation of the numerical model

Fish-like swimming involves the transfer of momentum between the fin and the surrounding water. The undulations of the fin push water backward, producing a jet. This phenomenon can be seen in Figures 11 (a) and (b), which represent the velocity field overlaid with the pressure field for anguilliform and gymnotiform swimming modes respectively at free-stream velocity $u_\infty = 3$ m/s, frequency of oscillation $f = 10$ Hz and amplitude $A_{max} = 0.02$ m. The instants represented are 0.25 t/T and 0.75 t/T, where t is the time and T is the oscillation period.

Figure 11 **Velocity field (m/s) overlaid with dynamic pressure field (Pa) at 0.25 *t/T* and 0.75 *t/T*; u_∞ = 3 m/s; *f* = 10 Hz and A_{max} = 0.02 m:**
(a) anguilliform swimming mode
(b) gymnotiform swimming mode
Slika 11 **Polje brzina (m/s) u zajedničkom prikazu s poljem dinamičkih tlakova (Pa) za 0,25 *t/T* i 0,75 *t/T*; u_∞ = 3 m/s; *f* = 10 Hz i A_{max} = 0,02 m:**
(a) način plivanja riba iz reda Anguilliformes
(b) način plivanja riba iz reda Gymnotiformes

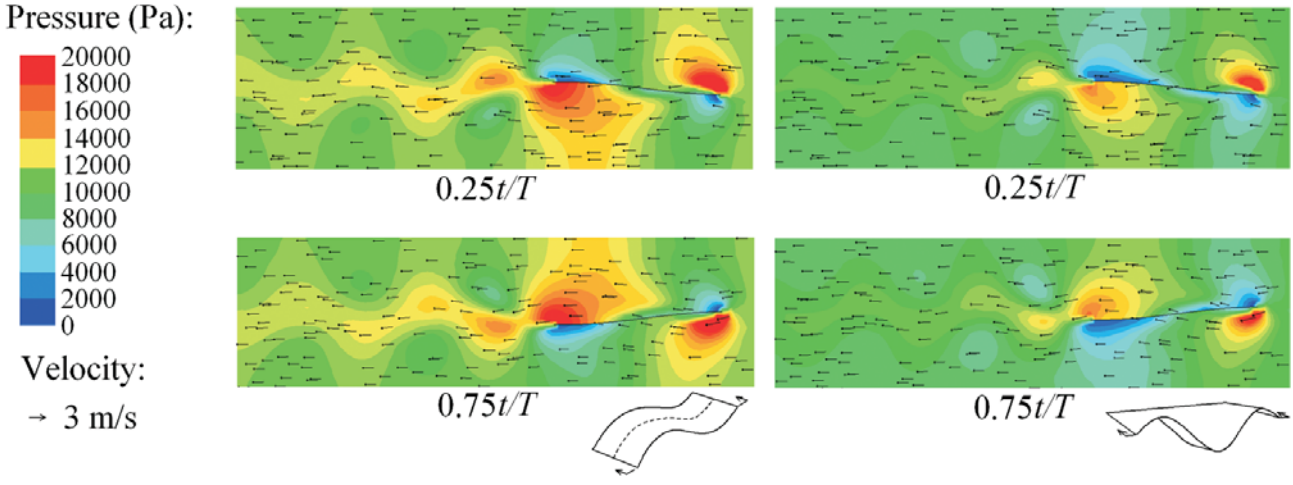

These pressure differences generate a pressure force, given by the following expression:

$$\vec{F}_p = -\int_s p\hat{n}dS \quad (1)$$

where p is the pressure, S the fin surface and $\hat{n}$ the vector normal to the fin surface. On the other hand, a viscous (friction) force, given by equation (2), arises as a result of the viscosity of water in the areas of flow with velocity gradients.

$$\vec{F}_v = \int_s \tau_{ij}\hat{n}dS \quad (2)$$

Figure 12 **Time variation of the x component of the average total force and instantaneous pressure, viscous and total forces at u_∞ = 3 m/s, f = 10 Hz and A_{max} = 0.02 m:**
(a) anguilliform swimming mode (accelerating)
(b) gymnotiform swimming mode (decelerating)

Slika 12 **Vremenska varijacija x komponente prosječne ukupne sile i trenutne vrijednost tlaka, viskozne i ukupne sile za u_∞ = 3 m/s, f = 10 Hz i A_{max} = 0,02 m:**
(a) način plivanja riba iz reda Anguilliformes (ubrzavajući)
(b) način plivanja riba iz reda Gymnotiformes (usporavajući)

(a)

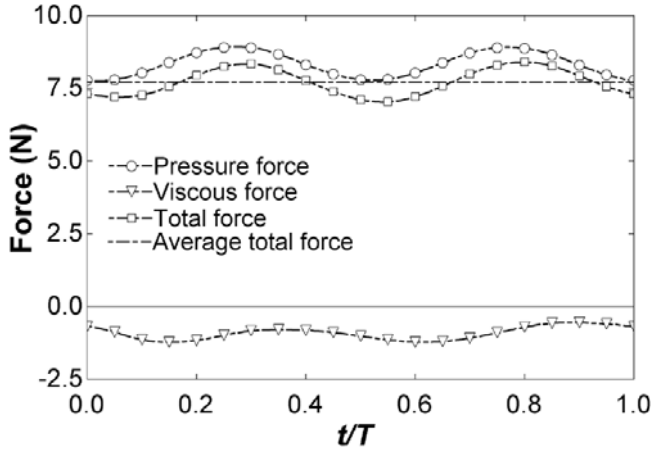

(b)

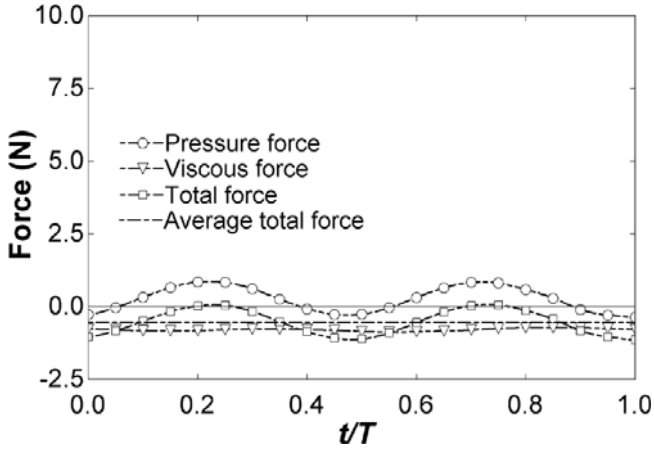

The total force is the sum of the pressure and viscous components. In the present work, only the x component (the component in the direction of the movement) is needed to produce thrust, given by:

$$F_x = F_{px} + F_{vx} \quad (3)$$

where F_{px} and F_{vx} are the x components of the pressure and viscous forces respectively.

The x components of these forces are shown in Figures 12 (a) and (b) for anguilliform and gymnotiform swimming modes respectively, at $u_\infty = 3$ m/s, $f = 10$ Hz and $A_{max} = 0.02$ m. The average total force per cycle is also represented in these figures.

Figure 13 **X component of the average forces against u_∞. f = 10 Hz, A_{max} = 0.02 m:**
(a) anguilliform movement
(b) gymnotiform movement

Slika 13 **X komponenta prosječnih vrijednosti sila u ovisnosti o u_∞. f = 10 Hz, A_{max} = 0,02 m:**
(a) način plivanja riba iz reda Anguilliformes
(b) način plivanja riba iz reda Gymnotiformes

(a)

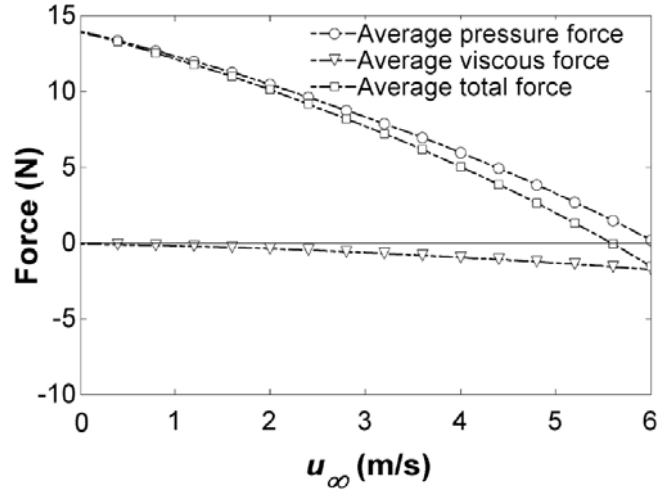

(b)

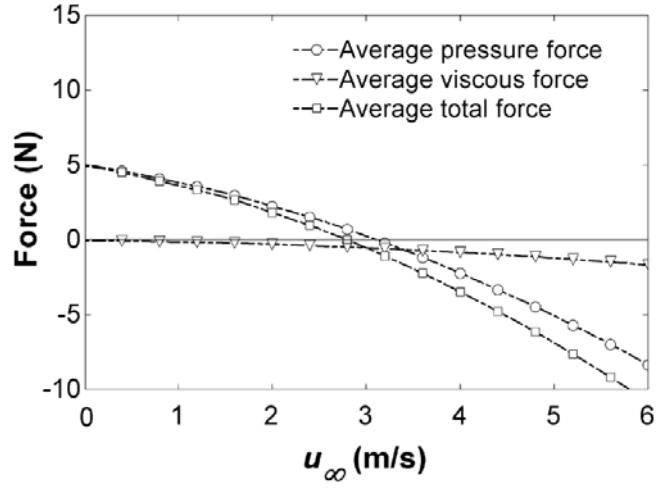

As seen in Figure 12, the pressure and viscosity forces in each cycle exhibit two peaks, corresponding to the forward and backward tail strokes. Under these conditions, anguilliform swimming mode produces a much higher pressure force and slightly higher viscous force than gymnotiform swimming mode. The average total force per cycle for anguilliform swimming mode is positive, which means that the fin is accelerating. On the contrary, this force is negative for gymnotiform swimming mode, which means that the fin is decelerating.

Figure 14 **X component of the average total force against frequency for numerical and experimental results; u_∞ = 0 m/s, and A_{max} = 0.02 m:**
(a) anguilliform swimming mode
b) gymnotiform swimming mode

Slika 14 **X komponenta prosječne vrijednosti ukupne sile u ovisnosti o frekvenciji za numerički i eksperimentalno dobivene rezultate; u_∞ = 0 m/s, and A_{max} = 0,02 m:**
(a) način plivanja riba iz reda Anguilliformes;
(b) način plivanja riba iz reda Gymnotiformes

(a)

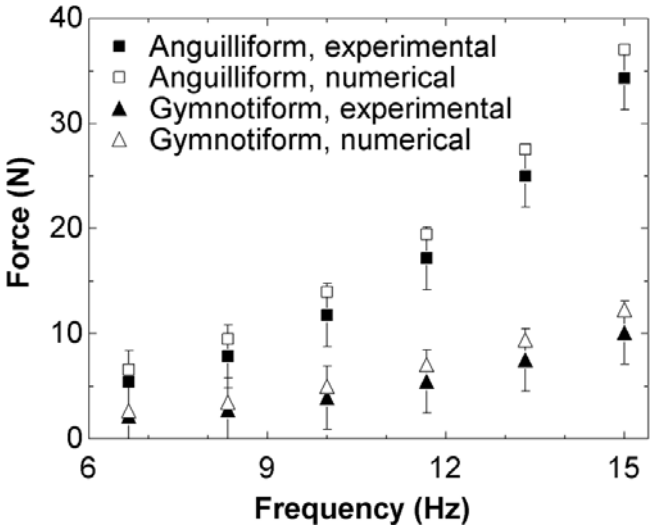

(b)

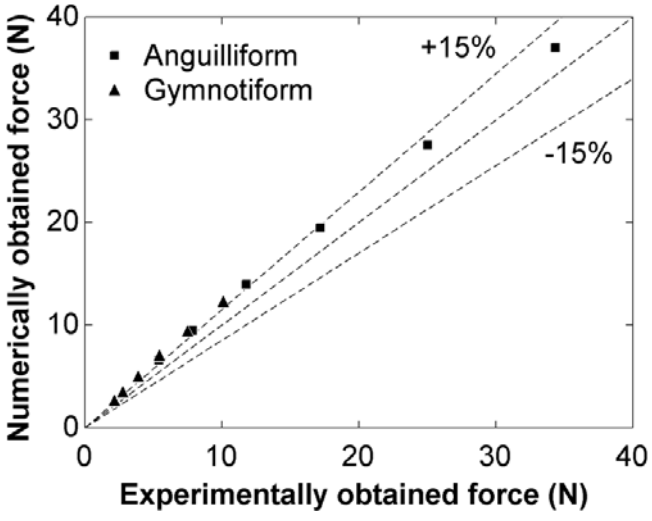

It is interesting to study the average forces per cycle against the free-stream velocity. This is shown in Figures 13 (a) and (b) for anguilliform and gymnotiform swimming modes respectively. As can be seen, when the free-stream velocity is zero, the pressure force is maximum and the viscous force is minimum. As the free-stream velocity is increased, the pressure force is reduced and the viscous force is slightly increased, until the free-steam velocity is such that the pressure force equals the viscous force and therefore the total force is zero. Under this condition, the fin swims at constant velocity, *i.e.*, there is neither acceleration nor deceleration. This cruising velocity is 5.5 m/s for anguilliform swimming mode and 2.8 m/s for gymnotiform swimming mode. If the free-stream velocity is higher than the cruising velocity, the fin decelerates.

The results obtained in the present work were validated with experimental data using the prototypes shown in Figures 6 and 8. Figure 14 (a) shows the average total force per cycle against the frequency of oscillation at $u_\infty = 0$ m/s and $A_{max} = 0.02$ m. As can be seen, the numerical results match well the experimental data, for both the anguilliform and gymnotiform swimming modes. Figure 14 (b) shows that the error is less than 15% in practically all the measurements. Once validated with experimental results, the numerical model was employed to study all the undulating fin patterns proposed in Figure 9 in the preceding section.

5.2 Efficiency, cruising velocity and power

When the x component of the total force (defined by equation (3)) is zero, the pressure force equals the viscous force. Under this condition, the useful power is the thrust (force) multiplied by the cruising velocity:

$$P_U = F_{px} u_\infty = F_{vx} u_\infty \tag{4}$$

The total power (the power consumed by the fin) is the sum of the useful power and the power expended to produce the oscillations, given by:

$$P_T = F_{px} u_\infty + \int_S p\vec{v}_{wall}\,\hat{n}dS \tag{5}$$

where p is the pressure and $\vec{v}_{wall}$ refers to the undulating velocity of the fin.

The efficiency is the ratio of useful power divided by the total power:

$$\eta = \frac{P_U}{P_T} \tag{6}$$

The cruising velocity (when the total force is zero), efficiency, useful power and total power are shown in Table 1. As can be seen, thunniform is the most efficient swimming mode and anguilliform is the fastest. Despite some superficial similarities with thunniform swimmers, ostraciiform locomotion has a lower efficiency and cruising velocity. Anguilliform swimming has lower efficiency than thunniform and caranguiform, because the undulation amplitudes along the entire body of anguilliform swimmers produce power that is wasted. On the contrary, in thunniform and caranguiform thrust practically takes part in the posterior half of the fin. Gymnotiform swimming mode is the slowest and least efficient for the parameters studied.

Table 1 **Cruising velocity and efficiency; f = 10 Hz and A_{max} = 0.02 m**
Tablica 1 **Brzina krstarenja i učinkovitost; f = 10 Hz i A_{max} = 0,02 m**

Fin movement	u_∞ (m/s)	η (%)	P_U (W)	P_T (W)
Anguilliform	5.5	31.1	8.2	26.3
Caranguiform	4.8	38.6	6.3	16.3
Thunniform	5.1	44.4	7.1	16.0
Ostraciiform	4.5	34.1	5.6	16.4
Gymnotiform	3.2	18.2	2.6	14.3

The cruising velocity and efficiency depend on the parameters of the problem and, in particular, on the oscillation frequency and maximum amplitude. These results are shown in Figures 15 and 16. As can be seen, the cruising velocity increases as the frequency increases, Figure 15 (a). On the other hand, the cruising velocity increases rapidly from zero to its maximum value and then decreases gradually with the increase of the frequency, Figure 15 (b). Concerning the amplitude, the cruising velocity increases as the amplitude increases, Figure 16 (a), but the efficiency decreases as the amplitude increases, Figure 16 (b). The reason is that the thrust is incremented at high amplitudes at the expense of even larger power cost required and hence less efficiency.

Figure 15 **Influence of the oscillation frequency: (a) on the cruising velocity; (b) on the efficiency; A_{max} = 0.02 m.**
Slika 15 **Utjecaj frekvencije oscilacije na: (a) brzinu krstarenja (b) na učinkovitost; A_{max} = 0,02 m.**

(a)

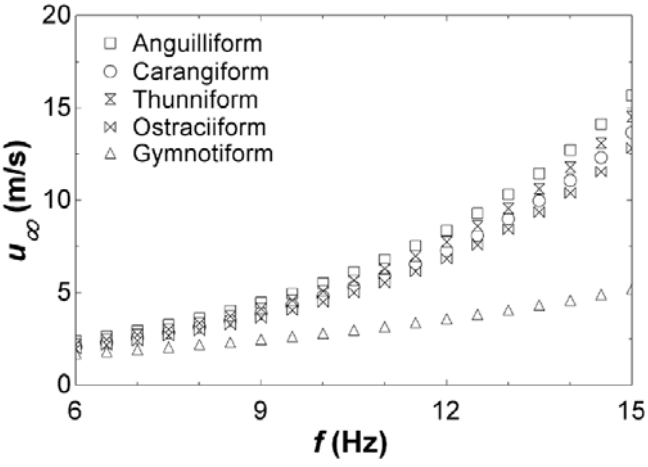

(b)

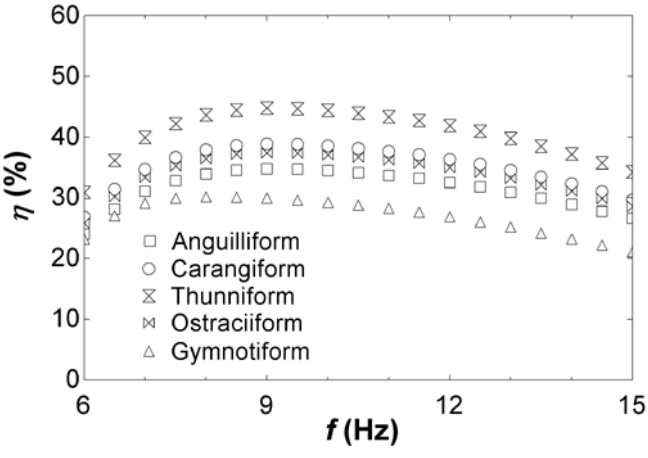

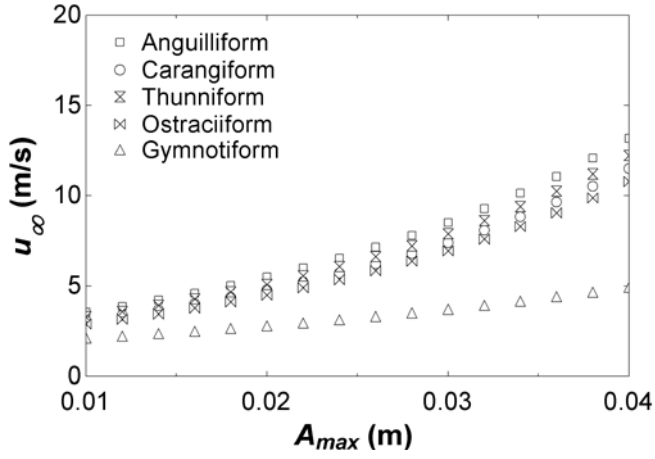

(a)

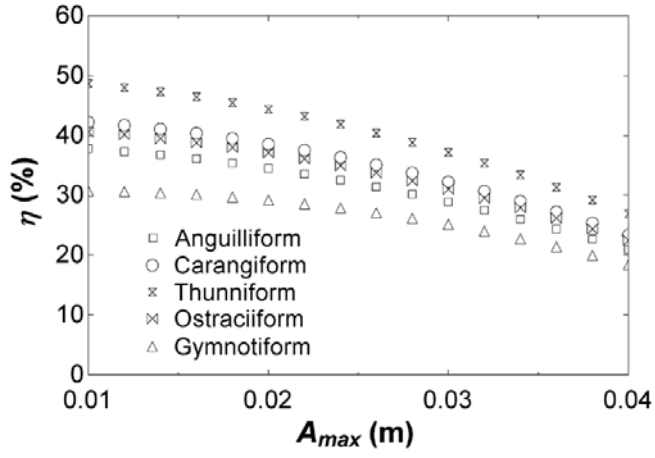

(b)

Figure 16 **Influence of the amplitude: (a) on the cruising velocity (b) on the efficiency; f = 10 Hz**
Slika 16 **Utjecaj amplitude na: (a) brzinu krstarenja (b) učinkovitost; f = 10 Hz**

6 Conclusions

This paper presents a CFD analysis of several biologically-inspired marine propulsors. The aim is to provide information for engineers with an interest in the emerging area of aquatic biomechanisms. Once validated with experimental results, the numerical model was employed to study one MPF and four BCF movements. The pressure and velocity fields were obtained, as

well as the hydrodynamic forces (which were decomposed into pressure and viscous forces), cruising velocity and efficiency. The results show that the fin pattern makes important influence on the performance, obtaining that thunniform swimming mode is the most efficient. Several values of the amplitude and frequency of oscillation were analyzed, obtaining that the efficiency and cruising velocity depend strongly on these parameters. From these results, the best option for marine propulsion should be a combination of thrust and efficiency, which depends on each practical case. Military applications require high velocity and most civil applications require high efficiency.

It is important to mention that a rectangular shape was used as undulating fin. Future work is needed to study other hydrodynamic shapes (most fish have a characteristic shape and a lunate tail). Until such work is completed, it is difficult to accurately judge which is the most efficient and fastest swimming mode. Nevertheless, the present work is an important step to understand biologically-inspired marine propulsion.

7 Acknowledgements

The authors gratefully acknowledge the financial support given to the investigation by the *Xunta de Galicia*, Spain, through the project PGIDIT06DPI172PR8.

8 Nomenclature

A	Amplitude, m
f	Oscillation frequency, Hz
F	Force, N
$\hat{\boldsymbol{n}}$	Unit normal vector
p	Pressure, Pa
S	Surface, m^2
t	Time, s
T	Period, s^{-1}
u	Velocity, m/s

Greek symbols

η	Efficiency
μ	Dynamic viscosity, Pa·s
τ_{ij}	Viscous stress tensor, N/m^2

Subscripts

max	Maximum
p	Pressure
T	Total
U	Useful
v	Viscosity
wall	Wall (fin)
x	x direction
∞	Free-stream

9 References

[1] YAMAMOTO, I., TERADA, Y., NAGARTAU, T. and IMAIZUMI, Y.: Propulsion system with flexible/rigid oscillating fin, IEEE Journal of Oceanic Engineering, Vol. 20(1), p. 23-30, 1995.

[2] BARRETT, D.S., TRIANTAFYLLOU, M. S., YUE D.K.P.: Drag reduction in fish-like locomotion, Journal of Fluid Mechanics, Vol. 392, No. 10, p. 183-212, 1999.

[3] KATO, N.: Control performance in the horizontal plane of a fish robot with mechanical pectoral fins, IEEE Journal of Oceanic Engineering, Vol. 25(1), p. 121 – 129, 2000.

[4] GUO, S.: A new type of fish-like underwater microrobot, IEEE/ASME Transactions of Mechatronics, Vol. 8, No. 1, 2003.

[5] HERR, H., DENNIS, B.: A Swimming Robot Actuated by Living Muscle Tissue, Journal of NeuroEngineering and Rehabilitation, 2004.

[6] MacIVER, M.A., FONTAINE, E., BURDICK, J.W.: Designing future underwater vehicles : principles and mechanisms of the weakly electric fish, IEEE Journal of Oceanic Engineering, Vol. 29, No. 3, 2004.

[7] CLARK, R.P., SMITS, A. J.: Thrust production and wake structure of a batoid-inspired oscillating fin, Journal of Fluid Mechanics, 562, p. 415-429, 2006.

[8] LOW, K.H.: Locomotion simulation and system integration of robotic fish with modular undulating fin, International Journal of Simulation, 7(8), p. 64-77, 2008.

[9] LAMAS, M.I., RODRÍGUEZ, J.D., RODRÍGUEZ, C.G., GONZÁLEZ, P.B.: Three dimensional CFD analysis to study the thrust and efficiency of a biologically-inspired marine propulsor, Polish Maritime Research, No. 1(68), Vol. 18, p. 10-16, 2011.

[10] SFAKIOTAKIS, M., LANE, D.M., DAVIES, J.B.C.: Review of fish swimming modes for aquatic locomotion, IEEE Journal of Oceanic Engineering, 24(2), p. 237-252, 1999.

[11] CHENG, J.Y., CHAHINE, G.L.: Computational hydrodynamics of animal swimming: boundary element method and three-dimensional vortex wake structure, Comparative Biochemistry and Physiology Part A, Vol. 131, p. 51-60, 2001.

[12] COLGATE, J.E.: Mechanics and control of swimming: a review, IEEE Journal of Oceanic Engineering, Vol. 29; No. 3, p. 660-673, 2004.